

# Quantitative expression profiling of identified neurons reveals cell-specific constraints on highly variable levels of gene expression

David J. Schulz<sup>†‡</sup>, Jean-Marc Goillard<sup>§</sup>, and Eve E. Marder<sup>§¶</sup>

<sup>†</sup>Biological Sciences, 218A LeFevre Hall, University of Missouri, Columbia, MO 65211; and <sup>§</sup>Volen Center and Biology Department, MS 013, Brandeis University, 415 South Street, Waltham, MA 02116

Contributed by Eve E. Marder, June 21, 2007 (sent for review May 15, 2007)

The postdevelopmental basis of cellular identity and the unique cellular output of a particular neuron type are of particular interest in the nervous system because a detailed understanding of circuits responsible for complex processes in the brain is impeded by the often ambiguous classification of neurons in these circuits. Neurons have been classified by morphological, electrophysiological, and neurochemical techniques. More recently, molecular approaches, particularly microarray, have been applied to the question of neuronal identity. With the realization that proteins expressed exclusively in only one type of neuron are rare, expression profiles obtained from neuronal subtypes are analyzed to search for diagnostic patterns of gene expression. However, this expression profiling hinges on one critical and implicit assumption: that neurons of the same type in different animals achieve their conserved functional output via conserved levels and quantitative relationships of gene expression. Here we exploit the unambiguously identifiable neurons in the crab stomatogastric ganglion to investigate the precise quantitative expression profiling of neurons at the level of single-cell ion channel expression. By measuring absolute mRNA levels of six different channels in the same individually identified neurons, we demonstrate that not only do individual cell types possess highly variable levels of channel expression but that this variability is constrained by unique patterns of correlated channel expression.

ion channels | neuronal identity | plasticity | stomatogastric | quantitative PCR

Animals contain many different kinds of neurons that can be superficially described in terms of their anatomical forms, the patterns of connections they make, the neurotransmitters they release, and their electrophysiological properties. In small invertebrate nervous systems, it is relatively easy to identify neurons unambiguously by using one or more of the above attributes. Likewise, certain vertebrate neurons, such as the Mauthner cell in fish and amphibians (1), are unambiguously identifiable, as a function of size and location. In large vertebrate brains with many neurons with similar properties, it can be quite difficult to identify neurons unambiguously, which has significantly impeded efforts to understand the neuronal circuits in larger brains. Consequently, there are now major efforts under way to use a combination of molecular, anatomical, and physiological methods to identify neurons in vertebrate brains and spinal cords (2–4). Nonetheless, it is not yet apparent which combinations of attributes are adequate to define neuronal identity.

There is a large literature on the expression of various transcription factors and other genes in determining neuronal identity during development (5–8). However, characterizing the molecular processes that determine the lineage of a cell may not provide sufficient insight into the molecular markers expressed by those neurons many years later, as they function in the adult brain.

The electrophysiological phenotype of adult neurons depends on the number and kind of its ion channels. Recent theoretical and experimental work has shown that similar patterns of activity can be produced by a variety of quantitative combinations of the maximal conductances for different ion channels (9–15) and that values of individual channel densities can vary severalfold across cells of the same type (12, 13, 16, 17).

If the expression of each ion channel gene is not controlled tightly, what rules ensure that neurons can maintain their characteristic electrophysiological identities over days, months, and years despite ongoing channel turnover? One possibility is a process by which electrical activity is homeostatically regulated to a target level of excitability (16, 18, 19). A second, not mutually exclusive, possibility is that neuronal identity is captured in the patterns of expression in multiple channel genes and that the outcome of these correlations ensures the appropriate levels of activity, even though the levels of any one of the ion channels can be quite variable.

In this work, we used single-cell quantitative PCR to quantify the expression of six different ion channel genes in six different classes of identified neurons from the crab stomatogastric ganglion (STG). We compared expression levels of each channel both within and across cell types and found that different sets of correlated gene expression are seen in each class of identified neuron. Therefore, we hypothesize that in the adult nervous system, cellular output is determined by characteristic sets of correlated expressions of ion channel genes, suggesting the presence of cell type-specific mechanisms for unique transcriptional coregulation among the same common pool of channel genes.

## Results

The STG of the crab, *Cancer borealis*, contains 26–27 neurons (20) that are identifiable on the basis of their anatomical projections (21). The STG generates two rhythmic motor patterns, the rapid pyloric rhythm and a slower gastric mill rhythm. Fig. 1A shows simultaneous intracellular recordings from four motor neurons during the pyloric rhythm. These recordings show the membrane potential trajectories and characteristic firing patterns of these four cell types. Each STG has two pyloric

Author contributions: D.J.S., J.-M.G., and E.E.M. designed research; D.J.S. and J.-M.G. performed research; D.J.S., J.-M.G., and E.E.M. analyzed data; D.J.S. and E.E.M. wrote the paper.

The authors declare no conflict of interest.

Freely available online through the PNAS open access option.

Abbreviations: GM, gastric mill; IC, inferior cardiac; LG, lateral gastric; LP, lateral pyloric; LPG, lateral posterior gastric; PD, pyloric dilator; STG, stomatogastric ganglion.

Data deposition: The sequences reported in this paper have been deposited in the GenBank database [accession nos. DQ103254 (*Cab-sha*), DQ103256 (*Cab-BKKCa*), DQ103255 (*Cab-shab*), DQ103257 (*Cab-IH*), EF089568 (*Cab-para*), and EF089569 (*Cab-shaw*)].

<sup>†</sup>To whom correspondence may be addressed. E-mail: SchulzD@missouri.edu.

<sup>¶</sup>To whom correspondence may be addressed. E-mail: marder@brandeis.edu.

© 2007 by The National Academy of Sciences of the USA

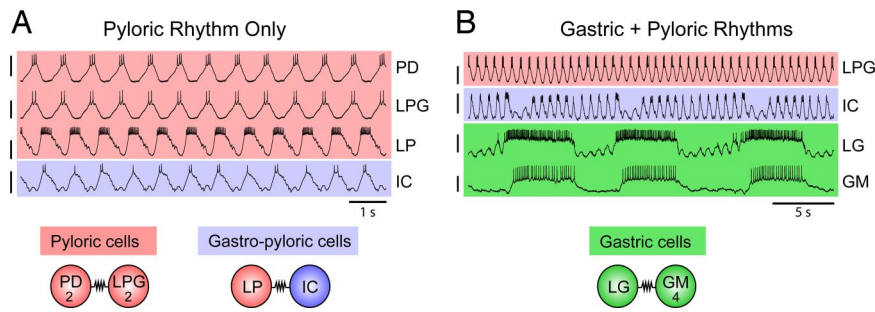


**Fig. 1.** Activity patterns of identified neurons in the STG in preparations showing only a pyloric rhythm, and both a gastric mill and pyloric rhythm. (A) Simultaneous intracellular recordings from PD, LP, LPG, and IC neurons during the ongoing pyloric rhythm. (Vertical scale bars:  $-40$  to  $-60$  mV.) (B) Simultaneous intracellular recordings from LPG, IC, LG, and GM cells during the ongoing pyloric and gastric rhythms. (Vertical scale bars:  $-40$  to  $-60$  mV.) Resistor symbols represent electrical synapses, and numbers noted with each cell type represent the number of cells of each type in one ganglion.

dilator (PD) and two lateral posterior gastric (LPG) neurons that are electrically coupled (Fig. 1) and fire synchronous bursts of action potentials during the pyloric rhythm. The single lateral pyloric (LP) and single inferior cardiac (IC) neurons are also electrically coupled and fire in the same phase of the pyloric rhythm (Fig. 1).

Fig. 1B shows four simultaneous intracellular recordings from the LPG, IC, lateral gastric (LG) (one in each STG) and gastric mill (GM) neurons (four in each STG) during an ongoing gastric rhythm. Note that the LPG neuron remains firing in time with the pyloric rhythm, whereas the electrically coupled (Fig. 1) LG and GM neurons fire in long, slow bursts characteristic of robust gastric activity. When the gastric rhythm is expressed, the IC neuronal activity reflects influences from both the pyloric and gastric rhythms. We chose these six neuron types for analysis because they included neurons from both rhythms and included neurons that were electrically coupled, both to other neurons of the same class, and to other cell types.

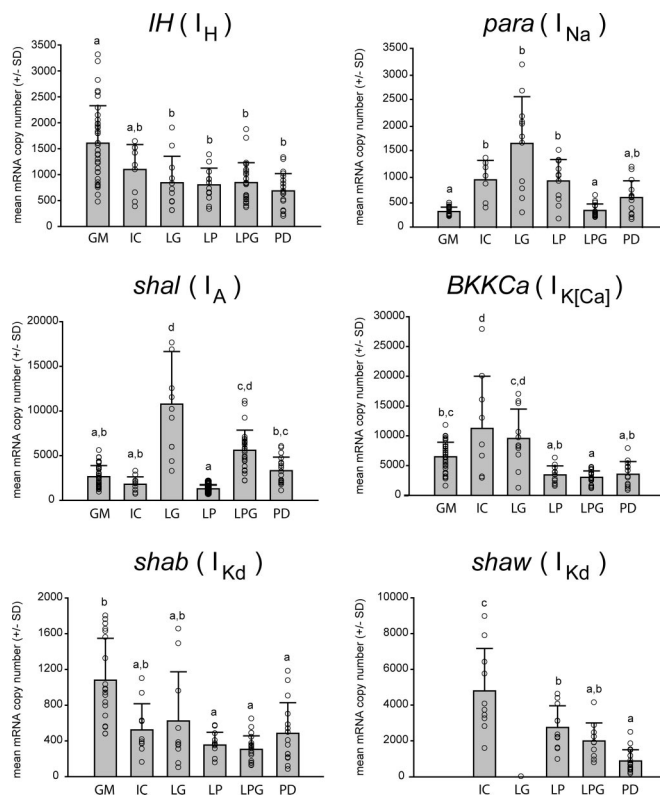
We measured the levels of mRNA expression for six different ion channels including four different  $K^+$  channels (*shal*  $I_A$ , *shab*  $I_{Kd}$ , *shaw*  $I_{Kd}$ , and *BKKCa*  $I_{K[Ca]}$ ), a hyperpolarization-activated inward current (*IH*  $I_H$ ), and a  $Na^+$  current (*para*  $I_{Na}$ ) in each of the six different cell types shown in Fig. 1. In these experiments, individual neurons were hand-dissected, and then quantitative real-time PCR was performed for multiple-channel genes on each neuron separately (12) (see *Experimental Procedures*).

Fig. 2 shows the raw data plus the mean  $\pm$  SD for all of the channels and cells used in this work. Mean levels of expression varied significantly among the cell types for each channel ( $P < 0.001$ , one-way ANOVA). Furthermore, the plotting of the individual data points shows the range of values over which each channel mRNA can vary in each neuron class. GM cells had the highest levels of expression of both *IH* and *shab* mRNA but the lowest mean levels of *para* expression. *Shaw* was not found in LG neurons. Because the relative levels of expression of these channels among cell types varied from channel to channel, these results demonstrate that there is not simply a scaling of expression with cell size or morphology. Rather, these results suggest that each cell type has a specific pattern of expression of channel mRNA that contributes to its unique functional identity.

By comparing the range of expression levels for six different channels in a given cell, it is clear that each cell type has a distinct pattern of expression. This phenomenon is illustrated in the three-dimensional plots in Fig. 3, which show that each cell type is found in a different region of the three-dimensional parameter spaces. Specifically, when mean distribution is plotted in three dimensions for three different channels (Fig. 3), each cell type is revealed to have a unique distribution of expression *shal* vs. *shab* vs. *shaw* and *para* vs. *BKKCa* vs. *IH* (two selected combinations of channel types). Taken together, these results demon-

strate that one can infer cell identity from examining the precise quantitative expression patterns of a small number of genes critical for the distinct output of a given cell type, in this case some of the ion channels that regulate cellular excitability.

Our results demonstrate not only that different types of neurons in the STG have unique quantitative patterns of ion channel expression, but they also support previous results (12, 22) that indicate that levels of expression of any given channel in a particular cell type can vary 3- to 5-fold (Fig. 2). To examine whether each individual cell arrives at the appropriate solution for functional output by stochastic variability of each ion channel



**Fig. 2.** Distinct patterns of ion channel expression are seen for each cell type. Mean  $\pm$  SD mRNA copy number for six different ion channels in each of the six cell types are overlaid with the individual data points that generate these means. Letters indicate significant differences ( $P < 0.05$ ) between cell types as revealed by pairwise post hoc comparisons (Tukey's  $t$  test) subsequent to a one-way ANOVA (each panel ANOVA results  $P < 0.05$ ). LG cells were not found to express measurable levels of *shaw*, whereas this transcript was not measured in GM cells.



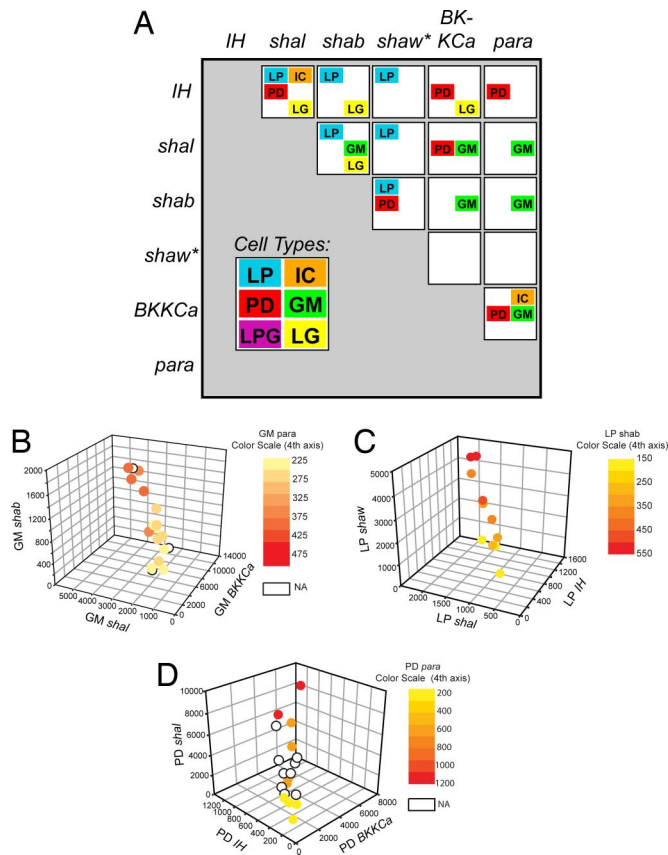


**Fig. 4.** Correlated levels of ion channel mRNA in specific STG cell types. (A) Summary of the coordinated expression of ion channels in six different cell types of the STG. Each box represents a possible pairwise correlation between two channels. Within each box, each cell type that was determined to have a significant pairwise correlation for ion channel mRNA levels is listed. \*, *shaw* mRNA was not detected in LG cells, and *shaw* was not quantified in GM cells. (B–D) Four-way correlations of ion channel expression in GM, LP, and PD cells. (B) Four-way plot of *shab* vs. *shal* vs. *BKCa* vs. *para* in GM neurons. mRNA Levels of *para* are expressed as increasing intensity of color from yellow to red as shown. (C) Four-way plot of *shaw* vs. *shal* vs. *IH* vs. *shab* in LP cells. (D) Four-way plot of *shal* vs. *IH* vs. *BKCa* vs. *para* in PD cells.

(23, 24) as well as variability in the regulatory sequences and transcriptional machinery leading to gene transcription (“extrinsic variability”) (25, 26). Although our work does not directly address the origin of the variability of gene expression between cells of the same type, our results cannot be explained by simple intrinsic variability. We showed that although the same identified neurons in different animals display 3- to 5-fold variability in the level of expression of any one ion channel, these expression levels are not independently variable, but show cell-specific correlations. Although compensatory changes in gene expression have been demonstrated previously between *shal* and *IH* (27, 28), our work reveals the potential extent to which channel genes are coregulated in neurons known to maintain constant function in the networks in which they function (29). We argue that cell identity is not a static result of gene expression, but rather a continual balance between compensatory changes in gene expression and coordinated gene regulation that ensures robust output.

Recent elegant studies have focused on complex gene networks as critical determinants of transcriptional regulation (30, 31), but a relatively limited number of regulators may act in a combinatorial fashion to influence transcription and ultimately neuronal identity (32). Therefore, in mature neurons, a combi-

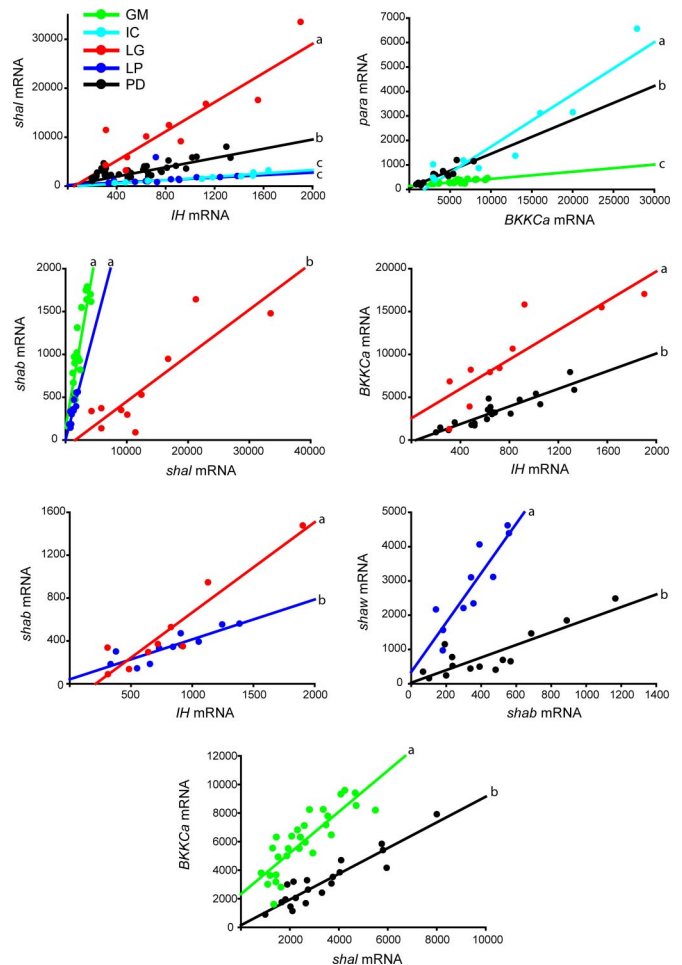


**Fig. 5.** Cells that share the same pairwise correlation among channels differ in the quantitative relationship between these channels. Each plot shows all of the cell types that share a common pairwise correlation between ion channels. Letters indicate significant differences between the slopes of the regression lines for each shared correlation.

natorial code of coregulated ion channel expression may exist that acts as the primary determinant of the output of a cell at any given time. Baumgardt *et al.* (32) suggest that the maintenance of this cellular output may require only a relatively few coordinating players acting in a combinatorial fashion, greatly reducing the complexity of feedback mechanisms (and the number of players involved) that would be required to coordinate channel expression in a cell-specific fashion to maintain appropriate neuronal output.

What might be the biochemical mechanisms behind the striking difference in putative coregulation of the same genes in different cell types (Fig. 3)? Two non-mutually exclusive possibilities seem most likely. One is that intrinsic differences exist between cell types in the transcription factors and/or microRNAs (miRNAs) that regulate mRNA levels for these genes. These intrinsic differences in abundance or activity of such factors presumably would be the result of developmental processes during determination of cell fate (33, 34). Alternatively, activity-dependent processes may exist that feed back to the transcription factors/miRNAs regulating ion channel gene expression (35–37). Because each cell type has a unique pattern of activity, these factors presumably would be differentially regulated by these activity-dependent processes, leading to differences in the relationship between channel genes in different cell types. As is often

the case in dynamic biological systems, the answer may lie in a combination of these two putative mechanisms.

### Experimental Procedures

Adult crabs, *C. borealis* ( $n = 20$ ), were obtained from Yankee Lobster (Boston, MA) and maintained in artificial seawater until used. Crabs were anesthetized by keeping them on ice for 30 min before dissection. The complete stomatogastric nervous system was dissected out of the animal and pinned out in a Sylgard-coated (Dow Corning, Midland, MI) dish containing chilled (12–13°C) physiological saline solution (440 mM NaCl/11 mM KCl/13 mM CaCl<sub>2</sub>/26 mM MgCl<sub>2</sub>/Tris/5 mM maleic acid, pH 7.45).

**Electrophysiology.** For electrophysiological recordings, the STG was desheathed, and petroleum jelly wells were placed on the motor nerves. Extracellular recordings from the nerves were made by placing stainless steel pin electrodes in the wells. Signals were amplified and filtered with a differential AC amplifier (A-M Systems, Carlsborg, WA). Intracellular recordings from the STG somata were made by using 20- to 40-M $\Omega$  glass microelectrodes filled with 0.6 M K<sub>2</sub>SO<sub>4</sub>/20 mM KCl and an Axoclamp 2A (Molecular Devices, Sunnyvale, CA). Pyloric motor neurons were identified with standard procedures for *C. borealis* (38, 39). During recordings, the preparations were superfused continuously with chilled (12–13°C) control physiological saline. Unless otherwise specified, chemicals were obtained from Sigma (St. Louis, MO). Data were acquired with a Digidata 1200 data acquisition board (Molecular Devices) and subsequently analyzed in Clampfit (version 9; Molecular Devices) or Spike2 (version 4; Cambridge Electronic Design, Cambridge, U.K.) with programs written in the Spike2 script language.

**Cloning of Ion Channel Genes from *C. borealis*.** In addition to using previously optimized real-time primers to quantify *shal*, *I<sub>H</sub>*, *shab*, and *BKCa*, we cloned and sequenced partial ORFs for two additional channels from the crab, *C. borealis*: *para* (I<sub>Na</sub>), and *shaw* (K<sub>v2</sub>), as described previously (12).

**Harvesting Individually Identified Neurons.** Individually identified neurons were harvested as described in detail elsewhere (12). Briefly, the cells were identified electrophysiologically, and the location within the ganglion of relevant cell somata was mapped. The cells were partially dissociated enzymatically, and the phys-

iological saline was replaced with 70% ethylene glycol, and the cells were frozen at –80°C for 1 h. Individual cell somata then were individually harvested by hand-held forceps while still cold and placed into 350  $\mu$ l of lysis buffer (buffer RLT as provided by Qiagen, Valencia, CA) containing 1% 2-mercaptoethanol and frozen at –80°C until RNA extraction.

**Quantitative Single-Cell RT-PCR.** Quantitative PCR was performed as described by Schulz *et al.* (12). Raw mRNA copy numbers for each channel from each cell then were normalized by comparing the 18S rRNA in each cell with the mean 18S levels of a population of neurons processed simultaneously. Primers specific for real-time PCR detection of *shal*, *BKCa*, *shab*, *shaw*, *I<sub>H</sub>*, *para*, and 18S rRNA using Sybr Green were developed and designed by using Primer3 software. The sequences of primers were as follows: *Shal* forward, 5'-CTACATCGGTCTTGGCATCA-3'; *Shal* reverse, 5'-AGATCCTGAACACGCGAAAC-3'; *BK-Kca* forward, 5'-TAAGCTGTGTTTCATGCTGG-3'; *BK-Kca* reverse, 5'-GCAGCCATCATGTTCTG-3'; *Shab* forward 5'-AAGTTAGCCCGACACTC-GAC-3'; *Shab* reverse 5'-ATTAACACGCCCATGGCTAA-3'; *I<sub>H</sub>* forward, 5'-GAACGGGTATCATGCAACAA-3'; *I<sub>H</sub>* reverse, 5'-TCTAGTGGCACCGAGGAGAT-3'; 18S forward, 5'-AGGTATGCGCTACAATGG-3'; 18S reverse, 5'-GCTGCCTCCT-TAGATGTGG-3'; *Para* forward, 5'-TCGGTATGGTGTCT-GAAGGAT-3'; *Para* reverse, 5'-CAGTGTTCGGATACCCT-TGG-3'; *Shaw* forward, 5'-CGATAGGCATCCAGGAGTGT-3'; *Shaw* reverse, 5'-TACTCCAGCTCCTCCTCGAA-3'.

**Statistical Analyses.** Statistical analyses were performed with SPSS version 13.0 (SPSS, Inc., Chicago, IL) and Prism version 4.03 (GraphPad, San Diego, CA). Significant pairwise correlations among ion channels were determined by using Pearson's correlation coefficient. Differences in mean expression levels of each channel among different cell types were determined with one-way ANOVA and post hoc *t* tests (Tukey's). Comparisons of the slopes of the same ion channel correlations in multiple cell types were performed with a modified form of analysis of covariance.

We thank Chris Johnson for help obtaining the cells used in this work. This work was supported by National Institutes of Health Grant MH-46742 (to E.E.M.), the McDonnell Foundation (to E.E.M.), National Science Foundation Grant IOB-0615160 (to D.J.S.) and startup funds from the University of Missouri-Columbia (to D.J.S.).

1. Fetcho JR (1991) *Brain Behav Evol* 37:298–316.
2. Nelson SB, Sugino K, Hempel CM (2006) *Trends Neurosci* 29:339–345.
3. Sugino K, Hempel CM, Miller MN, Hattot AM, Shapiro P, Wu C, Huang ZJ, Nelson SB (2006) *Nat Neurosci* 9:99–107.
4. Markram H, Toledo-Rodriguez M, Wang Y, Gupta A, Silberberg G, Wu C (2004) *Nat Rev Neurosci* 5:793–807.
5. Lanuza GM, Gosgnach S, Pierani A, Jessell TM, Goulding M (2004) *Neuron* 42:375–386.
6. Lewis KE, Eisen JS (2003) *Prog Neurobiol* 69:419–449.
7. Millan KJ, Millonig JH, Hatten ME (2004) *Dev Biol* 270:382–392.
8. Wonders CP, Anderson SA (2006) *Nat Rev Neurosci* 7:687–696.
9. Goldman MS, Golowasch J, Marder E, Abbott LF (2001) *J Neurosci* 21:5229–5238.
10. Golowasch J, Goldman MS, Abbott LF, Marder E (2002) *J Neurophysiol* 87:1129–1131.
11. Prinz AA, Bucher D, Marder E (2004) *Nat Neurosci* 7:1345–1352.
12. Schulz DJ, Goaillard JM, Marder E (2006) *Nat Neurosci* 9:356–362.
13. Swensen AM, Bean BP (2005) *J Neurosci* 25:3509–3520.
14. Tobin AE, Calabrese RL (2006) *J Neurophysiol* 96:2089–2106.
15. Achard P, De Schutter E (2006) *PLoS Comput Biol* 2:e94.
16. Liu Z, Golowasch J, Marder E, Abbott LF (1998) *J Neurosci* 18:2309–2320.
17. Golowasch J, Abbott LF, Marder E (1999) *J Neurosci* 19:RC33.
18. LeMasson G, Marder E, Abbott LF (1993) *Science* 259:1915–1917.
19. Turrigiano GG, Nelson SB (2004) *Nat Rev Neurosci* 5:97–107.
20. Kilman VL, Marder E (1996) *J Comp Neurol* 374:362–375.
21. Maynard DM, Dando MR (1974) *Philos Trans R Soc London B* 268:161–220.
22. Baro DJ, Levini RM, Kim MT, Willms AR, Lanning CC, Rodriguez HE, Harris-Warrick RM (1997) *J Neurosci* 17:6597–6610.
23. Ozbudak EM, Thattai M, Kurtser I, Grossman AD, van Oudenaarden A (2002) *Nat Genet* 31:69–73.
24. Raser JM, O'Shea EK (2005) *Science* 309:2010–2013.
25. Blake WJ, Kærn M, Cantor CR, Collins JJ (2003) *Nature* 422:633–637.
26. Volfson D, Marciniak J, Blake WJ, Ostroff N, Tsimring LS, Hasty J (2006) *Nature* 439:861–864.
27. MacLean JN, Zhang Y, Goeritz ML, Casey R, Oliva R, Guckenheimer J, Harris-Warrick RM (2005) *J Neurophysiol* 94:3601–3617.
28. MacLean JN, Zhang Y, Johnson BR, Harris-Warrick RM (2003) *Neuron* 37:109–120.
29. Bucher D, Prinz AA, Marder E (2005) *J Neurosci* 25:1611–1619.
30. Fraser AG, Marcotte EM (2004) *Curr Opin Genet Dev* 14:336–342.
31. Ochoa-Espinosa A, Small S (2006) *Curr Opin Genet Dev* 16:165–170.
32. Baumgardt M, Miguel-Aliaga I, Karlsson D, Ekman H, Thor S (2007) *PLoS Biol* 5:e37.
33. Colvis CM, Pollock JD, Goodman RH, Impey S, Dunn J, Mandel G, Champagne FA, Mayford M, Korzus E, Kumar A, *et al.* (2005) *J Neurosci* 25:10379–10389.
34. Conaco C, Otto S, Han JJ, Mandel G (2006) *Proc Natl Acad Sci USA* 103:2422–2427.
35. Flavell SW, Cowan CW, Kim TK, Greer PL, Lin Y, Paradis S, Griffith EC, Hu LS, Chen C, Greenberg ME (2006) *Science* 311:1008–1012.
36. Tang H, Goldman D (2006) *Proc Natl Acad Sci USA* 103:16977–16982.
37. Tao X, West AE, Chen WG, Corfas G, Greenberg ME (2002) *Neuron* 33:383–395.
38. Hooper SL, O'Neil MB, Wagner RJ, Ewer J, Golowasch J, Marder E (1986) *J Comp Physiol A* 159:227–240.
39. Weimann JM, Meyrand P, Marder E (1991) *J Neurophysiol* 65:111–122.